



Sweroside Alleviated Aconitine-Induced Cardiac Toxicity in H9c2 Cardiomyoblast Cell Line

Li-Qun Ma^{1†}, You Yu^{2†}, Hui Chen², Mei Li², Awais Ihsan³, Hai-Ying Tong⁴, Xian-Ju Huang^{2,5*} and Yue Gao⁶

¹ College of Life Sciences, South-Central University for Nationalities, Wuhan, China, ² College of Pharmacy, South-Central University for Nationalities, Wuhan, China, ³ Department of Biosciences, COMSATS University Islamabad (CUI), Sahiwal, Pakistan, ⁴ School of Traditional Chinese Medicine, Beijing University of Chinese Medicine, Beijing, China, ⁵ National Demonstration Center for Experimental Ethnopharmacology Education, South-Central University for Nationalities, Wuhan, China, ⁶ Department of Pharmacology and Toxicology, Beijing Institute of Radiation Medicine, Beijing, China

OPEN ACCESS

Edited by:

Sanjoy Ghosh,
University of British Columbia
Okanagan, Canada

Reviewed by:

Jia-bo Wang,
302 Military Hospital of China, China
Yi Yang,
Guangzhou University of Chinese
Medicine, China

*Correspondence:

Xian-Ju Huang
xianju@mail.scuec.edu.cn

[†]These authors have contributed
equally to this work

Specialty section:

This article was submitted to
Ethnopharmacology,
a section of the journal
Frontiers in Pharmacology

Received: 10 April 2018

Accepted: 19 September 2018

Published: 25 October 2018

Citation:

Ma L-Q, Yu Y, Chen H, Li M, Ihsan A,
Tong H-Y, Huang X-J and Gao Y
(2018) Sweroside Alleviated
Aconitine-Induced Cardiac Toxicity
in H9c2 Cardiomyoblast Cell Line.
Front. Pharmacol. 9:1138.
doi: 10.3389/fphar.2018.01138

Aconitine is the main bioactive ingredient of Aconitum plants, which are well-known botanical herbs in China. Aconitine is also notorious for its high cardiotoxicity, as it can induce life-threatening ventricular arrhythmias. Unfortunately, there are few effective antidotes to aconitine toxicity. This study aimed to evaluate the potent protective effects of the ingredients from *V. baillonii* on aconitine toxicity on H9c2 cell line. Cell viability was assessed by methylthiazolotetrazolium bromide (MTT). Intracellular Ca²⁺ concentration alteration and reactive oxygen species (ROS) generation were observed by confocal microscopy and flow cytometry, respectively. Cellular oxidative stress was analyzed by measuring malondialdehyde (MDA) and superoxide dismutase (SOD) levels. Mitochondrial membrane potential ($\Delta\Psi$) was determined using JC-1 kit. RT-PCR and Hoechst staining techniques were conducted to determine the levels of autophagy/apoptosis. The mRNA levels of dihydropyridine receptor (DHPR), ryanodine receptors (RyR2) and sarcoplasmic reticulum Ca²⁺-ATPase (SERCA) were measured by RT-PCR. We screened six components from *V. baillonii*, among which, sweroside exhibited the strongest protective effects on aconitine-induced cardiac toxicity. Sweroside suppressed the aconitine-induced mRNA expressions of Na_v1.5 (encoded by SCN5A), RyR2 and DHPR, and reversed the aconitine-induced decrease in mRNA level of SERCA, thus preventing the aconitine-induced persistent intracellular Ca²⁺ accumulation and avoiding intracellular Ca²⁺ overload. We further found that sweroside restabilized the aconitine-disrupted mitochondrial membrane potential ($\Delta\Psi$) and reversed the aconitine-induced increase in the mRNA levels of cell autophagy-related factors (Beclin-1, Caspase-3, and LC3- II) in H9c2 cells. In the whole-animal experiments, we observed that sweroside (50 mg/kg) alleviated effectively aconitine-induced arrhythmias by analysis of electrocardiogram (ECG) recording in rats. Our results demonstrate that sweroside may protect cardiomyocytes from aconitine toxicity by maintaining intracellular Ca²⁺ homeostasis, restabilizing mitochondrial membrane potential ($\Delta\Psi$) and avoiding cell autophagy/apoptosis.

Keywords: aconitine, sweroside, cardiac toxicity, calcium overload, reactive oxygen species

INTRODUCTION

Aconitum plants, have been extensively used for centuries as traditional herbal medicines for a wide range of human maladies including rheumatism, inflammation in oriental countries. Aconitine is the main pharmacological ingredient in Aconitum plants. Despite the therapeutic benefits, aconitine is one of known cardiotoxins and neurotoxins (Honerjager and Meissner, 1983; Catterall et al., 1992; Ameri, 1998; Chan, 2009), it can cause lethal malignant ventricular arrhythmias. Aconitine and its analogs have even been developed into the experimental tools to establish cardiac arrhythmic models in modern heart research (Herzog et al., 1964; Sato et al., 1979; Hikino et al., 1980; Fraser et al., 2003). In clinic, herb-induced aconitine poisoning occur from time to time, as the narrow therapeutic index (Lin et al., 2004). However, the detoxification strategies for aconitine are still limited to supportive treatment, such as gastric lavage, charcoal hemoperfusion, catheterization, injection of atropine, or magnesium sulfate, and so on (Lin et al., 2004; Gottignies et al., 2009; Clara et al., 2015). Although, amiodarone was reported to successfully treat the aconitine-induced life-threatening arrhythmias, lidocaine and other classic antiarrhythmic drugs failed (Yeih et al., 2000), the paucity of effective and specific agents for aconitine poisoning is obvious. The aconitine toxicity, thus, needs a more detailed investigation to develop more effective and safe antidotes.

Veratilla baillonii Franch (*V. baillonii*) belongs to the family of Gentianaceae (Figure 1A). It is an ethnodrug that has long been used in the Southwest of China (Yang and Zhou, 1980). Local clinical evidence has indicated that *V. baillonii* possesses multiple pharmacological potential, as diverse as antipyretic, anti-inflammation and curing gastrospasm. Local people also believe that *V. baillonii* has preventative effects on toxicity from aconitum plants (Yang and Zhou, 1980). Our previous studies further supported this belief, as we observed that aconitine *in vivo* damaged the heart, liver, kidney and brain in rat, but the water extract of *V. baillonii*, which contains abundant iridoids (Huang et al., 2016), could attenuate the pathological changes of both acute (Ge et al., 2016) and subacute (Yu et al., 2016) toxicities induced by *Aconitum brachypodum* Diels (*A. brachypodum*). However, whether this protective action is mediated by these iridoids and the clear molecular mechanism remain to be elucidated.

Here, in this study, we evaluated the detoxication effects of active components from *V. baillonii* on aconitine-induced H9c2 cell injury, and the mechanism was explored in details. Three iridoids, gentiopicroside, and sweroside, swertiamarin, and three veratrilosides I, II, and III, were selected to evaluate their influences on cell activity by MTT assay and by measuring the lactate LDH release. The most promising active chemical was

then determined. Flow cytometry and real-time PCR were used to further elucidate the mediation of autophagy, intracellular calcium ions, intracellular ROS, and oxidative stress induction. Whole animal experiments were performed to test whether the compounds possess potential anti-arrhythmia effects in aconitine-induced arrhythmia rat model.

We found that sweroside, one of the iridoids from *V. baillonii*, exhibited protective effects on cardiomyocytes against aconitine toxicity, and maintaining intracellular Ca^{2+} homeostasis and avoiding cell autophagy/apoptosis may be involved in this protection.

MATERIALS AND METHODS

Guideline Statement

All methods used in this study are in accordance with protocols approved by the South-Central University for Nationalities. All animal studies comply with the Guide for the Ethical Committee in South-Central University for Nationalities (number of authorization: SYXK20 08-0 0 05).

Materials

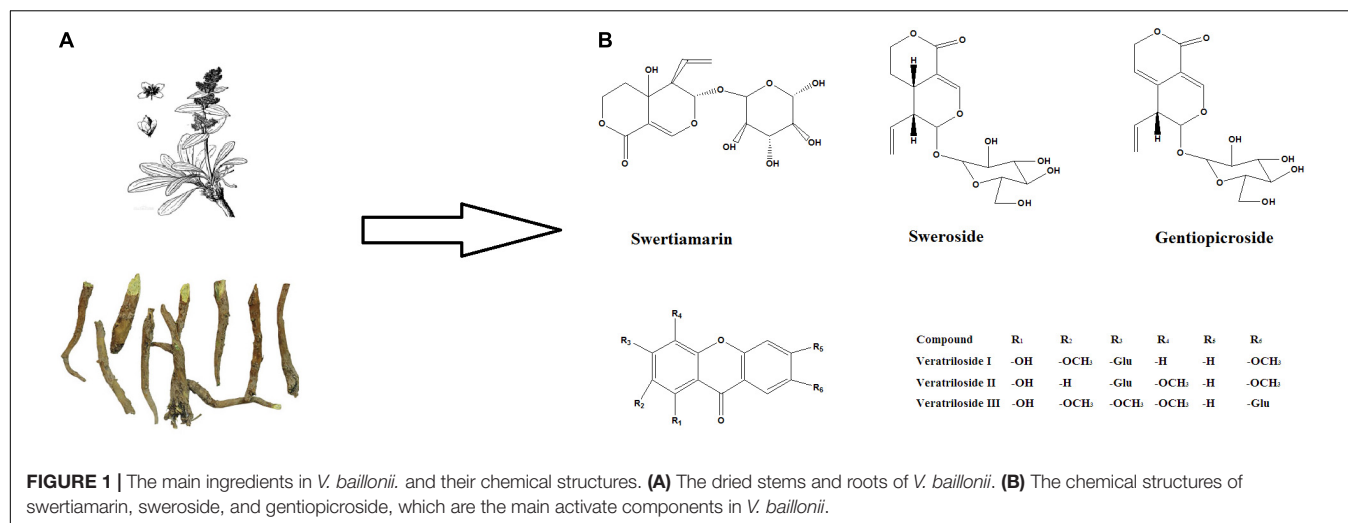
Aconitine was purchased from Sigma-Aldrich (Sigma-Aldrich, St. Louis, MO, United States). Secoiridoids of gentiopicroside, sweroside and swertiamarin were obtained from Yuanye Bio-Technology Co, Ltd (Shanghai, China). Veratriloside I, II, and III were extracted by our laboratory (Huang et al., 2016). The purities of the above substances were >98% as determined by HPLC-UV. All the compounds were dissolved in DMSO and then diluted in Dulbecco's modified Eagle's medium (DMEM, Hyclone, Logan, UT, United States) to the desired concentrations. The final concentration of DMSO was 0.1% (v/v) (Figure 1B).

Cell culture reagent of high glucose Dulbecco's modified Eagle's medium (DMEM) was purchased from Hyclone (Logan, United States). Trypsin was purchased from Biosharp (Anhui, China), and fetal bovine serum (FBS) was provided by Sijiqing Co. Ltd. (Hangzhou, China). The detection kit of 2', 7'- dichlorodihydro-fluorescein diacetate (DCFH-DA) was purchased from Sigma-Aldrich (St. Louis, MO, United States). The cell-permeable calcium-sensitive fluorescent dye Fluo-3/AM was purchased from Beyotime Institute of Biotechnology (Shanghai, China). Fluro-4/AM was purchased from Invitrogen (Camarillo, CA, United States).

Cell Cultures and Treatment

H9c2 cells, the rat cardiomyoblast cell line were obtained from Chinese Academy of Sciences Cell Bank (Shanghai, China). The cells were cultured in DMEM supplemented with 10% FBS, penicillin (100 U/mL) and streptomycin (100 μ g/mL) in a 5% CO_2 incubator at 37°C. The cell suspension (1×10^5 cells/ml) was plated into 96 well-plates and subcultured to 60~75% confluence for the following experiments. Different concentrations of the sample were prepared in serial dilutions, and DMSO (0.1%) was used as the control. H9c2 cells were underwent following treatments: (1) 0.01~50 μ M aconitine for 24 h, and then 10 μ M aconitine for the subsequent experiments;

Abbreviations: ECG, electrocardiogram; DHPR, dihydropyridine receptor; DMSO, dimethyl sulfoxide; LDH, lactate dehydrogenase; MDA, malondialdehyde; MTT, methylthiazolotetrazolium bromide; PVC, premature ventricular complex; ROS, reactive oxygen species; RyR2, ryanodine receptor; SERCA, sarco/endoplasmic reticulum Ca^{2+} -ATPase; SOD, superoxide dismutase; *V. baillonii*, *Veratilla baillonii* Franch; Vf, ventricular fibrillation; VT, ventricular tachycardia; WVBF, water decoction of *Veratilla baillonii*.



(2) 0~50 μM iridoidglucosides and 10 μM aconitine; (3) 0~50 μM Xanthones for 2 h, and then 10 μM aconitine exposure for 24 h.

Assessment of Cell Viability

Cell survival was observed using a phase-contrast microscope (OLYMPUS, Japan), and the cell viability was evaluated by the reduction of MTT and LDH release. Briefly, H9c2 cells (1×10^5 cells/ml) were treated with the suggested concentrations of the chemicals for the indicated time at 37°C. After 4 h of incubation with MTT (0.5 mg/ml), the cells were lysed in DMSO and the amount of MTT formazan was qualified by determining the absorbance at 570 nm using a microplate reader (Thermo Fisher 1510, United States). The cell viability was expressed as a percent of the control culture value. The level of LDH was detected with a commercially available kit according to the manufacturer's instruction (Jiancheng Bioengineering Institute, Nangjing, China). The absorbance was measured at 450 nm with a microplate reader as described above. LDH release (% of total) was calculated as the percentage of LDH in the medium vs. the total LDH activity in the cells.

Measurement of MDA Production and SOD Activity

The MDA contents and SOD activity were determined using commercial kits (Nanjing Jiancheng Bioengineering Institute, Nanjing, China) according to the manufacturer's instruction. To calculate the concentration of MDA and SOD, the protein concentrations of lysis buffer were measured by an enhanced bicinchoninic acid (BCA) protein assay kit (Beyotime Institute of Biotechnology, Shanghai, China).

Morphological Assessment of Apoptosis

Apoptosis was determined by incubating the cells with 10 $\mu\text{g}/\text{mL}$ Hoechst 33258 for 30 min at 37°C using the Hoechst staining kit (Beyotime Institute of Biotechnology, Shanghai, China) according to the manufacturer's protocol. Nuclear morphological changes in the cells were observed under an Olympus

fluorescence microscope (Tokyo, Japan) at a 461 nm emission. The apoptotic cells appeared with strong blue fluorescence, while the normal cells appeared with only weak fluorescence.

Measurement of Mitochondrial Membrane Potential ($\Delta\Psi$)

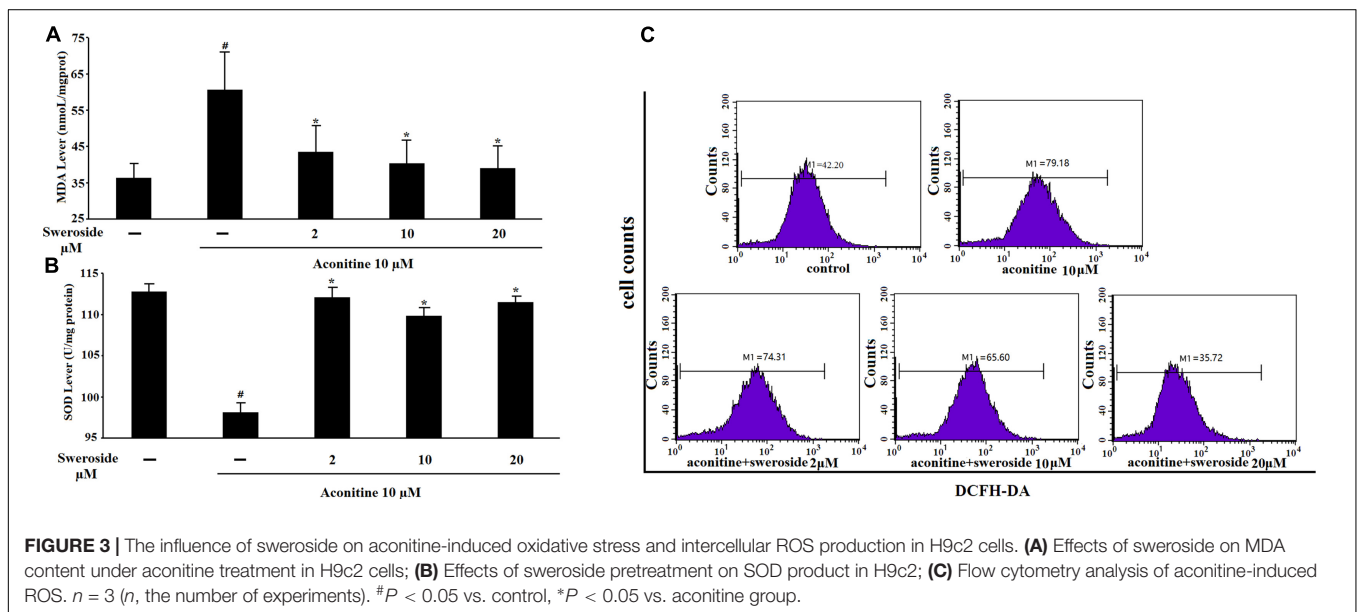
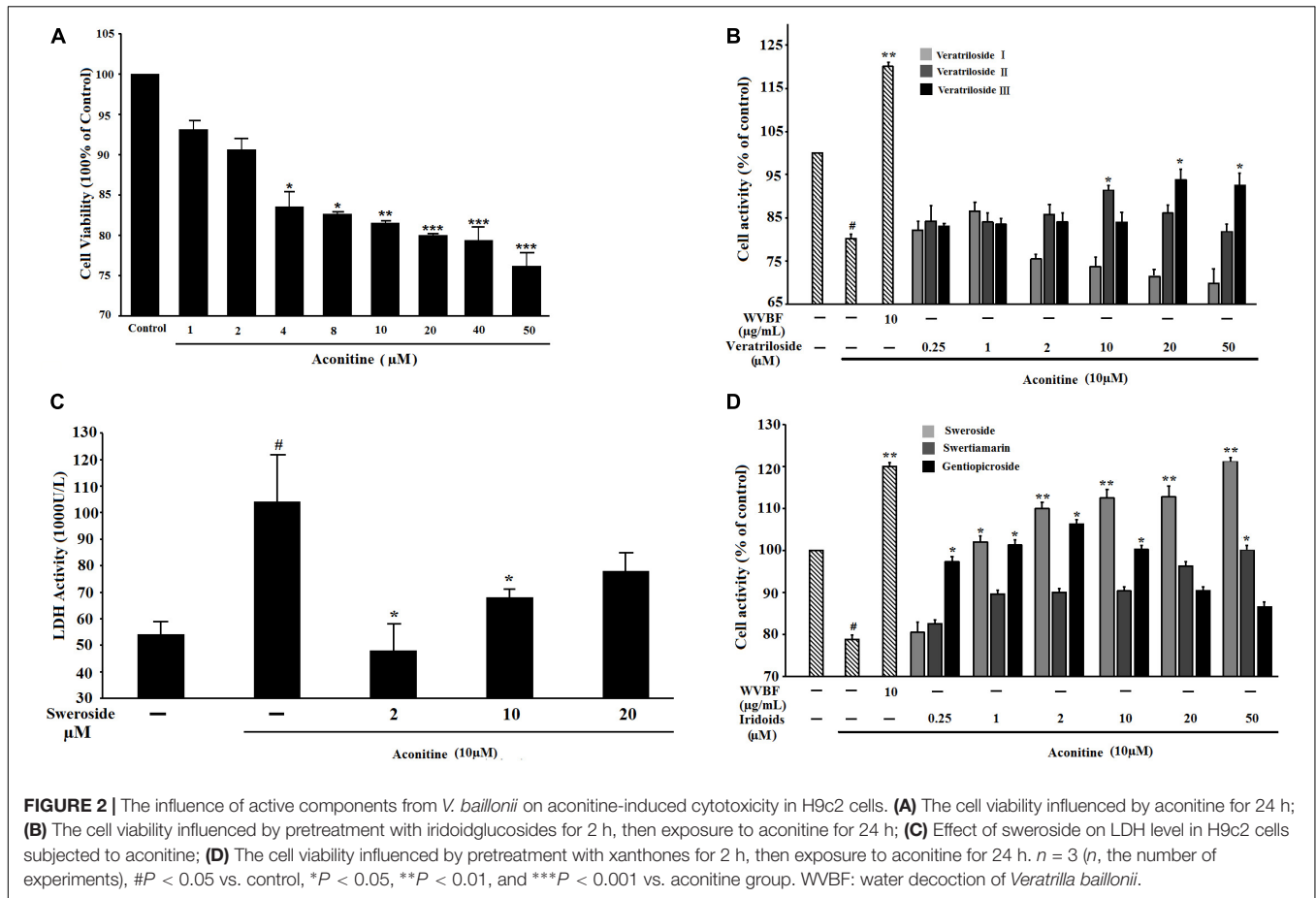
The change in the mitochondrial membrane potential ($\Delta\Psi$) was determined using the JC-1 kit (Beyotime Institute of Biotechnology, Shanghai, China). H9c2 cells from different treatment groups were washed with DMEM and incubated with JC-1 (1 μM) in DMEM at 37°C for 20min. After washing with DMEM, the cells were immediately detected by flow cytometry. The ratio of aggregated and monomeric JC-1 was used to quantify the change of $\Delta\Psi$. A decreased JC-1 ratio represents the depolarization of the mitochondria, indicating a decrease in $\Delta\Psi$.

Flow Cytometry for the Analysis of Intracellular ROS Generation

Dichloro-dihydro-fluorescein diacetate fluorescent probe was employed to monitor intracellular ROS. Cells in logarithmic growth phase were incubated in 6-well plates for 24 h for stabilization, then the medium was replaced with those containing 10 $\mu\text{mol}/\text{L}$ aconitine or aconitine

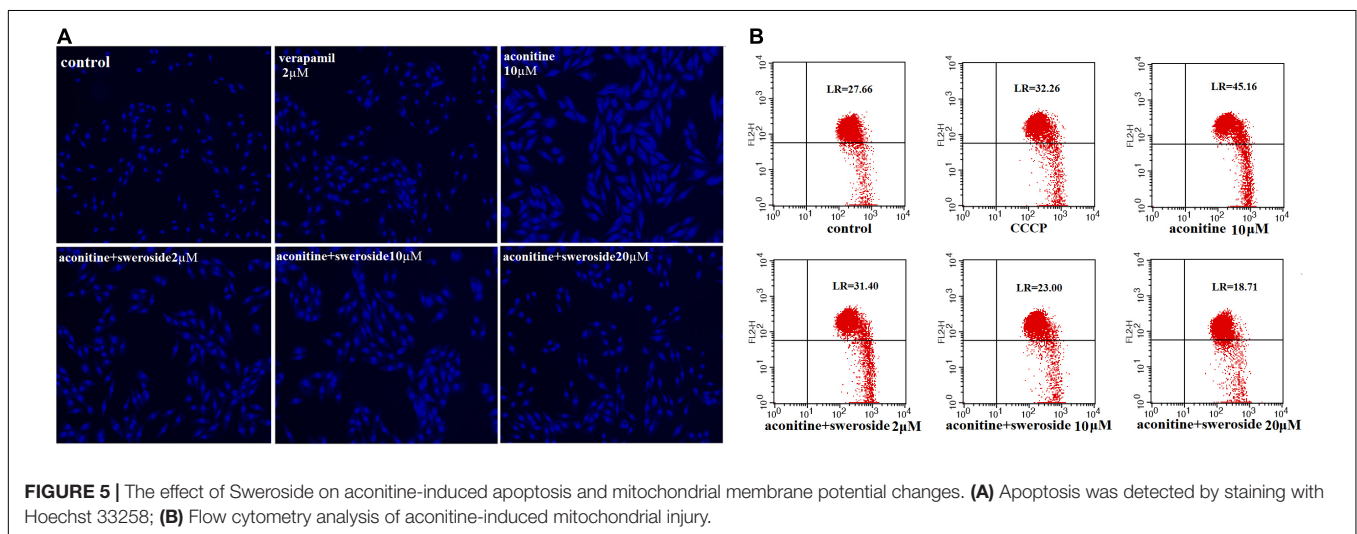
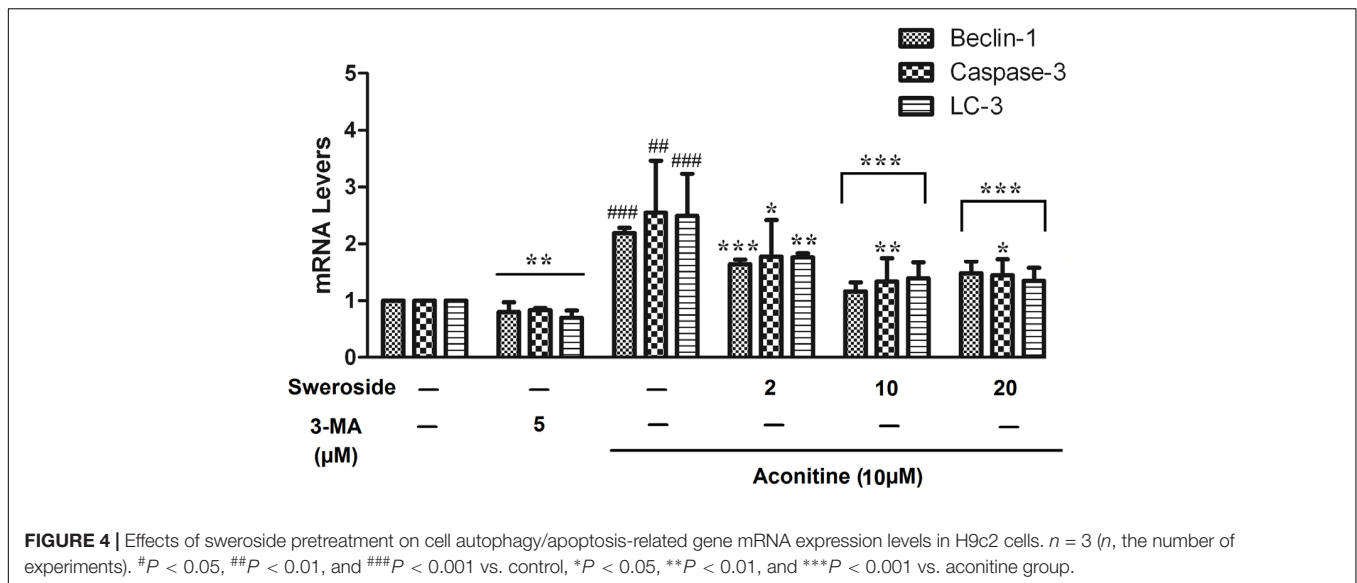
TABLE 1 | Primer sequences used for the amplification of target genes.

Gene	Forward	Reverse
GAPDH	TGTGTCGGTCGTGGATCTGA	TTGCTGTTGAAGTCGAGGAG
Beclin-1	GCCTCTGAAACTGGACACG	CCTCTTCTCCTGGCTCTCT
Caspase-3	GGAGCAGTTTTGTGTGTGTGA	AGTTTCGGCTTTCCAGTCAG
LC-3	ACCCTCTACGATGCTGGTGA	GCTGTCTCAATGTCTTCTG
DHPR	CATCTTTGGATCCTTTTTCGTTCT	TCCTCGAGCTTTGGCTTCTC
RyR2	TGCTGCGAGCCGGG	TGGCGGTGGCGTAGGA
SERCA2a	CAGCCATGGAGAACGCTCA	TCGTTGACCCCGAAGTGG
SCN5A	CACCCTCAACCTCTTCATCG	CTTCTTCTGCTCCTCCGTCA



(10 $\mu\text{mol/L}$)+sweroside (2–20 μM) for 24 h to observe the effects. After exposure, the cells were washed with fresh DMEM three times, and then they were resuspended at a concentration of 1×10^6 cells/ml and incubated with 10 μM DCFH-DA at

37°C for 30 min before being detected and analyzed by flow cytometry. A minimum of 20,000 events were analyzed per sample and the results were expressed as the fold-change of the fluorescence intensity over the control.



Measurement of Intracellular Ca^{2+} Levels by Flow Cytometry and Confocal Microscopy

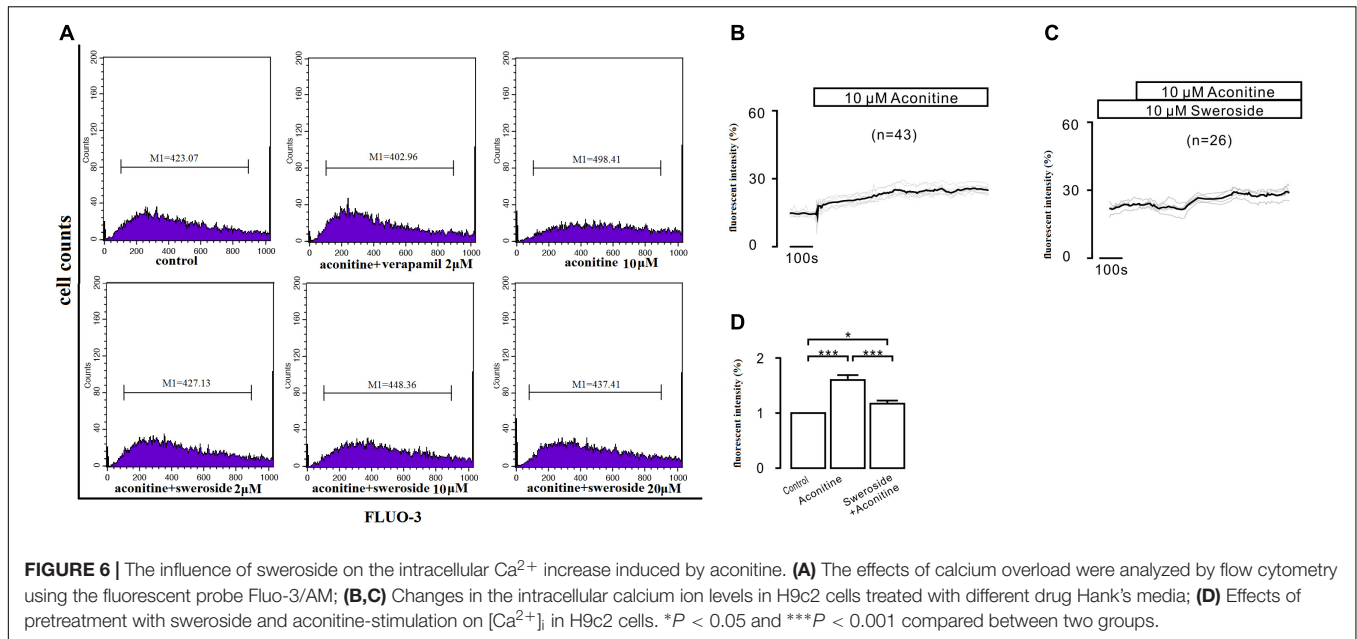
Employing Ca^{2+} indicators, Fluo-4/AM and Fluo-3/AM, to measure the intracellular Ca^{2+} concentrations ($[\text{Ca}^{2+}]_i$). Briefly, the cells in logarithmic growth phase were seeded in 6-well plates and incubated for 24 h for stabilization, then the medium was replaced with those containing 10 $\mu\text{mol/L}$ aconitine or aconitine (10 $\mu\text{mol/L}$)+sweroside (2–20 μM) and incubated for 24 h to observe the effects. After exposure, the cells were washed with fresh DMEM three times; then, the H9c2 cells were loaded with 5 $\mu\text{mol/L}$ Fluo-3/AM for 30 min at 37°C in dark. The fluorescence intensity was analyzed by flow cytometry.

In confocal experiments, H9c2 cells were seeded in circular discs and incubated with 10 μM sweroside for 2 h, then loaded with 2 μM Fluo-4/AM (dissolved in 0.1% DMSO plus pluronic acid (Life Technologies, Carlsbad, CA, United States) for 15 min

at 37°C in Tyrode's solution containing (in mmol/L): NaCl 143, KCl 5.4, CaCl_2 1.8, $\text{Na}_2\text{H}_2\text{PO}_4$ 0.3, MgCl_2 0.5, glucose 5.5, and HEPES 5, pH7.4 adjusted with 10M NaOH. The intracellular Ca^{2+} concentration was evaluated by measuring the fluorescence intensity excited at 488 nm and emitted at 510 nm using the LSM 700 Laser Confocal Microscopy System (Carl Zeiss, Berlin, Germany). The fluorescence was read every 5 s, and aconitine was administered into the discs at a fixed time point. The fluorescence intensity was determined before and after administrating drugs.

RNA Extraction and Real-Time Polymerase Chain Reaction (RT-PCR)

Real-time PCR was employed determine the gene expression. Briefly, the total RNA was extracted from H9c2 cells with the Trizol reagent (Qiagen, Valencia, CA United States). For mRNA quantification, cDNA was synthesized from 1 μg of total RNA using the PrimeScriptTM RT reagent kit (TaKaRa, Dalian,



China) following the manufacturer's instructions. Reactions were performed in a 20 μL volume according to the thermal cycler manufacturer's protocol (Rox) using an ABI 7500 Real-Time PCR system (Applied Biosystems) under the condition: 30 s at 95°C, followed by 40 cycles of 15 s at 95°C, and 34 s at 60°C (Ge et al., 2016). The primer sequences used for the amplification of target genes are listed in **Table 1**.

Animals and Administration of Drugs

Male Sprague-Dawley rats (200–250 g) were supplied by the Center of Laboratory Animals of Hubei Province (Wuhan, China).

A total of 30 rats were used in these serials of experiments. SD rats were randomly divided into three groups (6 for the control group, 12 for aconitine group, 12 for sweroside + aconitine group). The rats in control group received no treatment. The rats in sweroside + aconitine group received intraperitoneal injection (i.p.) of sweroside (50 mg/kg) for 5 days, once per day. Water and food were freely available for all of the animals.

ECG Recording

Pentobarbital sodium (3% dissolved in physiological salt; 90 mg/kg) was used for anesthesia. Standard Lead II ECG recording was carried out with a polygraph recorder (ADInstruments Pty Ltd, Australia). After a 15 min stabilization period, vehicle (i.e., physiological salt, i.p.) was administered to the control group, and aconitine (1 mg/kg, i.p.) were administered to induce arrhythmias in both aconitine group and sweroside + aconitine group. When the arrhythmias activity lasted and the ECG recording was continuously conducted 90 min post-administration. Data analysis was performed by using ECG Auto analysis software, Labchart Pro 8.

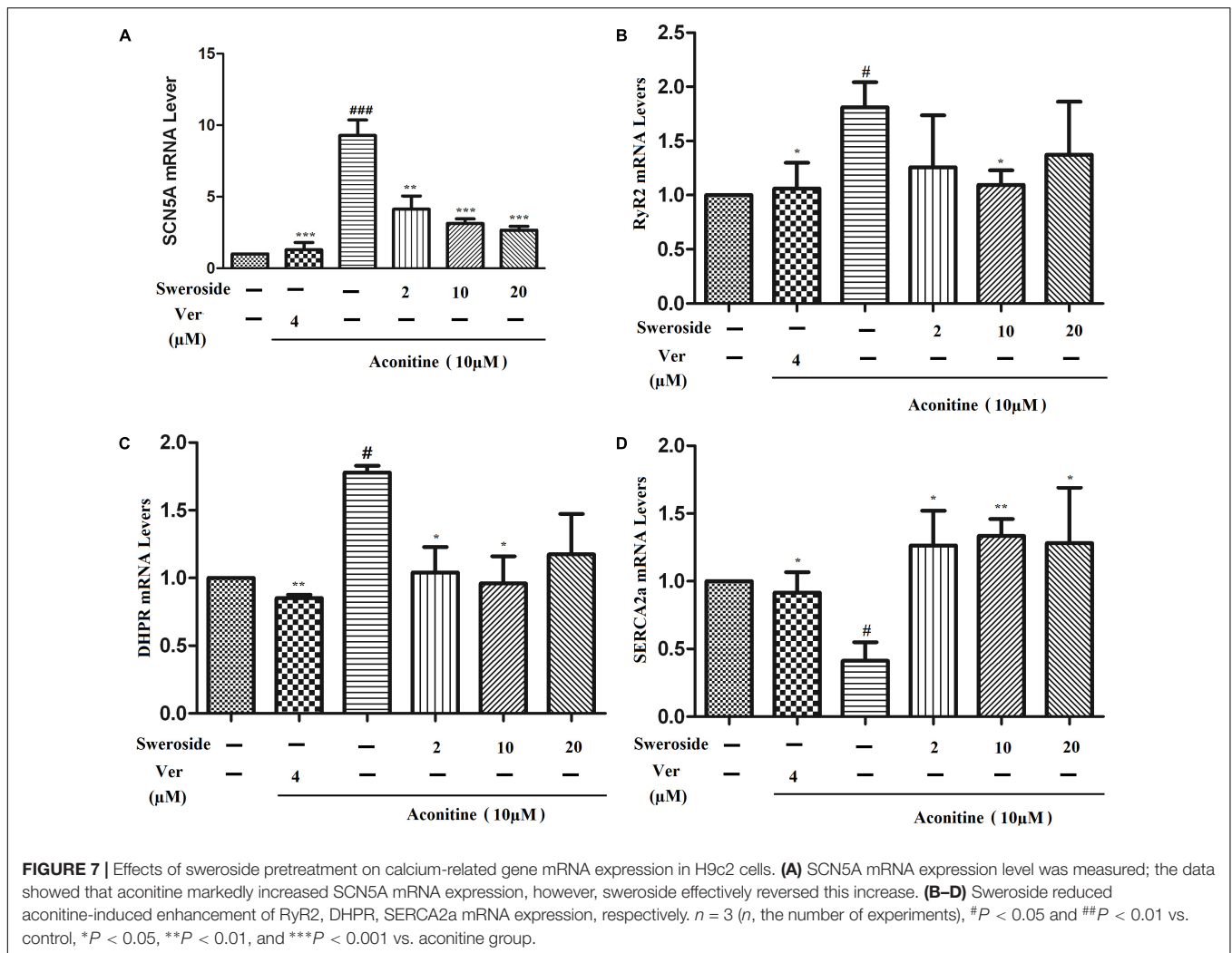
Statistical Analysis

All statistical analyses were performed in Origin 9.0 software (Origin Lab, Northampton, MA, United States). Data are presented as mean \pm standard deviation (SD) and were analyzed with one-way analysis of variance (ANOVA) or Student-Newman-Keuls test. $P < 0.05$ was considered statistically significant.

RESULTS

Sweroside Displayed Potential Protective Efficiency on Aconitine-Induced Cytotoxicity in H9c2 Cells

We first calculated the cytotoxicity of aconitine. As shown in **Figure 2A**, aconitine (4–50 μM) dose-dependently reduced the cell viability of H9c2 cells after incubation for 24 h. The IC_{50} value was 32 μM . Then, we screened six compounds and found that each of them could improve the cell survival, which had been reduced by 10 μM aconitine (**Figure 2B**) to varying degrees. Among these compounds, Veratrilosides I, II, and III showed weaker protection on H9c2 cells than WVBF (10 $\mu\text{g/ml}$) or secoiridoids. It was sweroside that exhibited the greatest efficiency among them (**Figure 2D**), so in the subsequent experiments, we explored its protective activity and the underlying mechanism in detail. 2 μM sweroside initiated the significant increase in the cell viability ($P < 0.01$ vs. aconitine group), and the efficiency reached its maximum at a concentration of 50 μM , a level similar to that of WVBF (10 $\mu\text{g/ml}$). Since LDH is widely used as a marker of cellular damage, the cell injury was assessed by determining LDH activity. The LDH leakage increased markedly in the aconitine group compared with the control group, but this increase was significantly blocked by sweroside treatment (2–10 μM) in a



dose-dependent manner (Figure 2C). Together, these findings indicated that sweroside could promote cell survival and reduce cell damage in H9c2 cells subjected to aconitine.

Sweroside Pretreatment Reduced Aconitine-Induced Oxidative Stress and Intercellular ROS Production in H9c2 Cells

Oxidative stress is one of the direct drivers of cell damage, it is an increase in the cellular and tissue concentrations of reactive oxygen species (ROS) due to peroxidation. We tested the level of lipid peroxidation by measuring the MDA level, which is the end product of lipid peroxidation. As illustrated in Figure 3A, the exposure of the cells to 10 μM aconitine resulted in a significant increase of the MDA level ($P < 0.05$) compared to that of control cells. This increase in the content of MDA induced by aconitine was blocked significantly by pretreatment the cells with sweroside (2, 10, 20 μM) ($P < 0.05$) (Figure 3A).

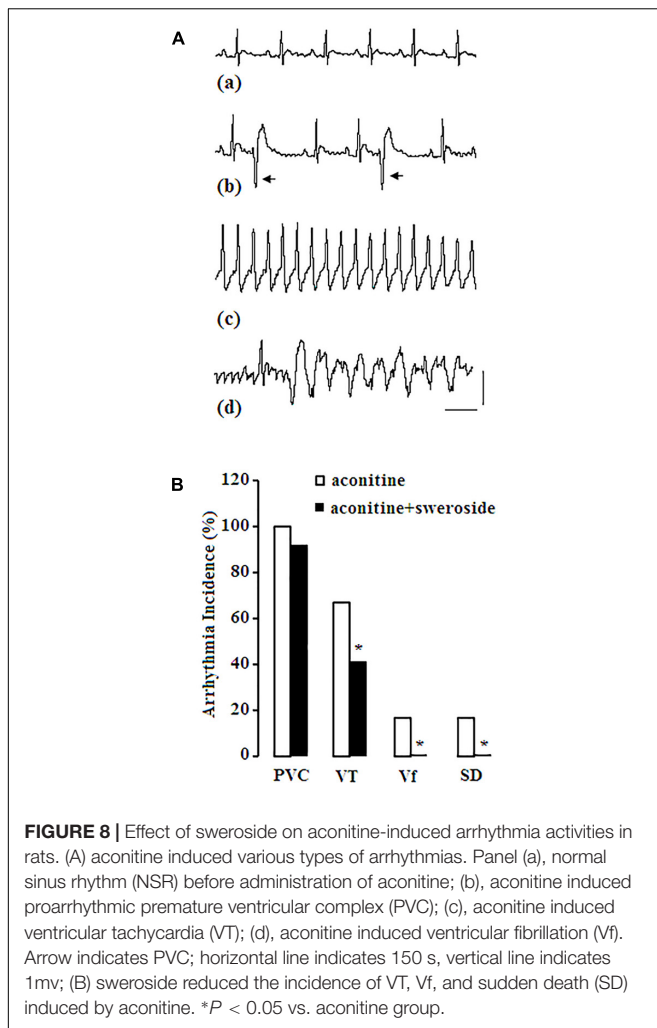
The effect of sweroside on the intracellular ROS production induced by aconitine was shown in Figure 3C. The cells

incubated with aconitine produced stronger DCF signals than the control group. However, incubation with both aconitine and a set of concentrations of sweroside (2–20 μM) resulted in a marked reduction in the DCF fluorescence (Figure 3C), indicating an inhibitory effect of sweroside on aconitine-induced intracellular ROS production.

The SOD activity was measured to further confirm the antioxidative ability of sweroside. As illuminated in Figure 3B, aconitine remarkably reduced the SOD activity, however, pre-incubation with sweroside significantly reversed this reduction ($P < 0.05$ vs. aconitine group).

Sweroside Inhibited the Increases in the mRNA Levels of Cell Autophagy/Apoptosis-Related Factors Induced by Aconitine in H9c2 Cells

To further study the protective effects of sweroside on aconitine-induced cardiac toxicity, a classical autophagy inhibitor, 3-methyladenine (3-MA), which is a phosphoinositide 3-kinase inhibitor that exerts its autophagy-inhibited effect before the



formation of the autophagosome was used as a pharmacological tool. LC3- II is a useful indicator of autophagosome initiation, and the LC3-II levels can rise with autophagy. As shown in **Figure 4**, aconitine could significantly increase the LC3-II and Beclin-1 mRNA levels (*P* < 0.01 vs. control group), indicating the inductive potential of autophagy; it could also lead to a marked increase of cleaved Caspase-3 mRNA levels as indicated (*P* < 0.01 vs. control group), suggesting its inductive potential for apoptosis. However, treatment with sweroside could substantially down-regulate all of these increased indexes induced by aconitine, which is a similar result to that of the positive control 3-MA. These results suggest that sweroside could protect cardiomyocytes via suppressing cell autophagy/apoptosis induced by aconitine.

Sweroside Prevented Aconitine-Induced Apoptosis Through Mitochondrion-Dependent Apoptotic Pathway

Normal living cells with Hoechst staining showed uniform blue fluorescence in the control group, while apoptotic cells showed

hyperchromatic and dense fluorescent particles within the massive apoptotic nuclear cytoplasm by fluorescence microscopy in the aconitine group. As shown in **Figure 5A**, sweroside could attenuate the cell apoptosis induced by aconitine.

The ultrastructural changes in H9c2 cells were examined to evaluate the myocardial damage induced by aconitine application. The control vs. sweroside group showed no significant difference. However, the proportion of the JC-1 monomer drastically increased in the group with aconitine application compared to the control; this increase was significantly blunted by sweroside pretreatment (**Figure 5B**). Mitochondrion is the key organelle mainly responsible for cell energy supply and cellular apoptosis. A decrease in the $\Delta\Psi$ causes membrane depolarization and triggers a cascade of apoptotic signaling (Hamacher-Brady et al., 2007). In the present study, JC-1 staining showed that sweroside pretreatment abated the aconitine-induced depolarization of the membrane potential in H9c2 cells (**Figure 5B**).

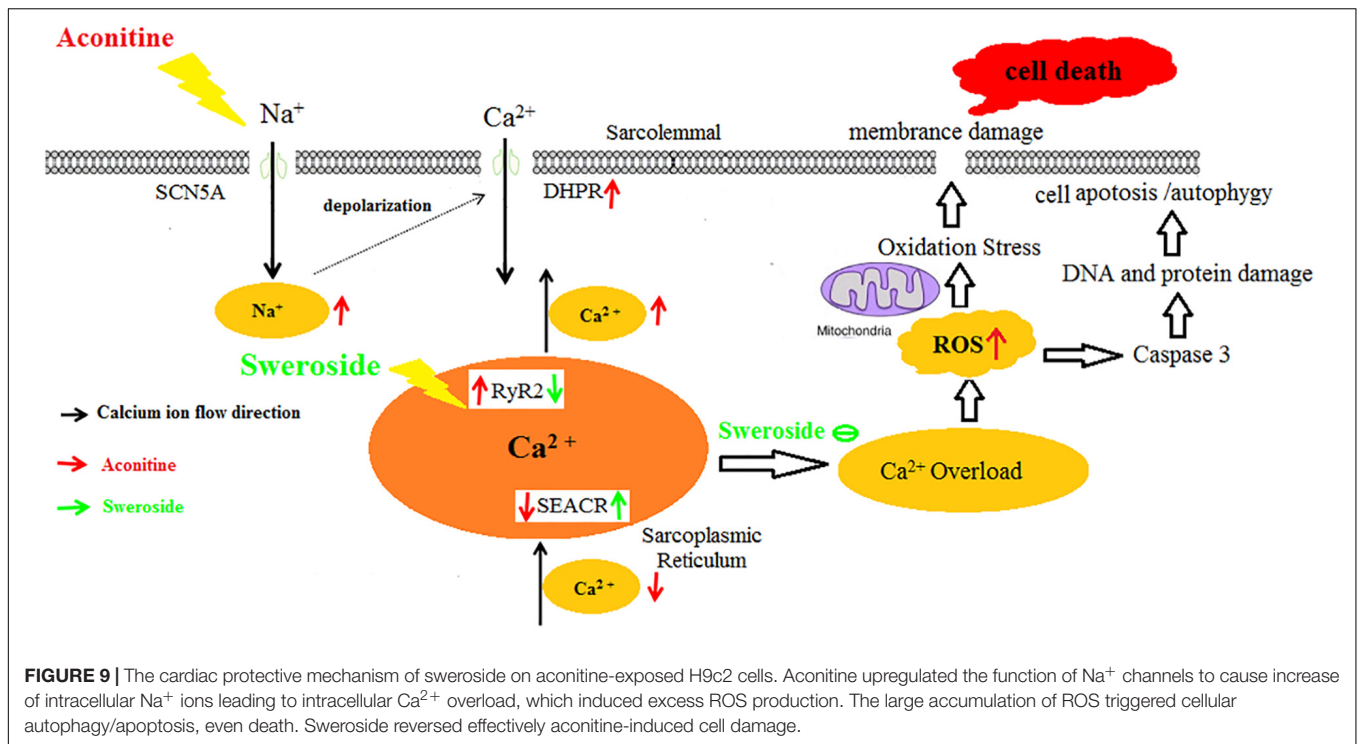
Sweroside Partially Blunted the Intracellular Ca^{2+} Increase Induced by Aconitine

As shown in **Figure 6A**, 10 μ M aconitine significantly potentiated Fluo-3 fluorescence, demonstrating an elevation in intracellular Ca^{2+} concentration. Sweroside (2–10 μ M) drastically inhibited this elevation of the intracellular Ca^{2+} .

To further validated the result above, we performed experiments to continually observe the dynamic changes of $[Ca^{2+}]_i$. The administration of 10 μ M aconitine led to a persistent and stable increase in $[Ca^{2+}]_i$ compared with that before the administration (*P* < 0.001), as shown in **Figure 6B**. However, pretreatment with sweroside for 2 h eliminated this aconitine-induced $[Ca^{2+}]_i$ elevation (**Figure 6C**). The fluorescence intensity changes coincide with the above description (**Figure 6D**).

Sweroside Reversed the Aconitine-Induced Changes of the mRNA Levels of DHPR, RyR2, and SERCA2a

The total RNA of the H9c2 cells was isolated and analyzed by semi-quantitative RT-PCR. Cells exposed to such dose showed significant differences between the aconitine group and the sweroside treatment group (**Figure 7**). The increased mRNA expression levels of DHPR, SCN5A and RyR2 in the aconitine group (*P* < 0.05) suggested that aconitine could up-regulate L-type voltage-dependent Ca^{2+} channels (LVDCCs), sarcoplasmic reticulum Ca^{2+} release channels and Na^+ channels. Aconitine exposure could moderately suppress SERCA2a mRNA level (*P* < 0.05), indicating that aconitine inhibited the activity of SERCA2a. The increased mRNA expression level of DHPR and RyR2 induced by aconitine were reversed almost completely by pretreatment with verapamil and sweroside, respectively, compared to the aconitine group (*P* < 0.05). Both verapamil and sweroside also noticeably recovered the aconitine-induced suppression of the SERCA2a expressions noticeably (*P* < 0.01),



suggesting that sweroside acts against the aconitine-induced stimulation on the cardiomyocytes ion channels.

Sweroside Ameliorated Aconitine-Induced Arrhythmias in Rats

Finally, we assessed whether prevention of sweroside on H9c2 cells could ameliorate cardiac arrhythmias induced by aconitine in rats. To test this hypothesis, we performed whole rat experiments. As shown in **Figure 8A**, in aconitine group, all of the rats were observed to occur proarrhythmic premature ventricular complex (PVC) during the ECG recording, 66.7% of rats developed into VT, 16.7% of which even rapidly deteriorated into Vf, subsequently, died. In sweroside treatment group, before aconitine administration, the ECG recording had no changes, compared with the control group (data not shown); after aconitine administration, the majority of rats occurred arrhythmias during the ECG recording, however, there was a significantly reduced incidence of VT, Vf, and sudden death (SD) compared with aconitine group (**Figure 8B**). Thus, sweroside ameliorated aconitine-induced ventricular arrhythmias and reduced the risk of death. In control group, there was no abnormality observed in ECG recording.

DISCUSSION

Although the cardiac toxicity of aconitine has been widely recognized (Honerjager and Meissner, 1983; Catterall et al., 1992; Ameri, 1998), there are few antidotes available to countact the deadly symptoms induced by aconitine or aconitum plants. In this study, we observed that aconitine caused severe cell damage

in H9c2 cell line, and sweroside strongly prevented the cells from such damage. These findings are consistent with our previous *in vivo* data (Yu et al., 2016). The aconitine-induced toxicity in H9c2 cells is characterized by increased oxidative stress, inducing autophagy/apoptosis, disturbing mitochondrion the potential and triggering Ca²⁺ overload.

Secoiridoids, a type of monoterpenes that has the general form of cyclopentanopyran with one of the rings open, are the characteristic components of the medicinal plants of the Gentianaceae family, which includes gentiopicroside, sweroside and swertiamarin (Herzog et al., 1964; Hikino et al., 1980; Honerjager and Meissner, 1983). The present results revealed that sweroside could remarkably attenuate the cell death/apoptosis of H9c2 cells induced by aconitine, suggesting that secoiridoids, especially sweroside, are the material basis of the therapeutic uses of *V. baillonii* for aconitine-induced toxicity. Other Gentianaceae plants containing secoiridoids may also demonstrate potent protective effect against the cardiac toxicity induced by aconitum medicine. However, the specific weight and the influences of the various secoiridoids remain unknown, which require further experimental confirmation in the future.

Calcium is one of the most crucial intracellular messengers, it functions to translate extracellular stimuli into intracellular signaling pathways that ultimately regulate cellular development, survival, differentiation and gene expression (Naranjo and Mellstrom, 2012). Therefore the intracellular calcium concentration must be precisely regulated to avoid cellular injury. This delicate calcium balance is maintained by Ca²⁺-permeable channels (mainly including DHPR and RyR2), calcium pumps, and exchangers (Berridge et al., 2000; Carafoli, 2002; Naranjo and Mellstrom, 2012). Any factors or stimuli

that disrupt this well-defined Ca^{2+} balance give rise to heart disease, including arrhythmia (Greiser and Schotten, 2013). This mechanism may be an important cause for the increased arrhythmias known to occur with aconitine toxicity. Aconitine increases the accumulation of intracellular Na^+ by up-regulation of the function of voltage-gated sodium channels, and inhibits SERCA2 expressions on the sarcoplasmic reticulum, leading to membrane depolarization (Sawanobori et al., 1987; Wright, 2002; Zhou et al., 2013). Such depolarization is expected to open DHPRs, resulting in Ca^{2+} influx into the cells, which then activates the RyR2 channels, leading to massive release of Ca^{2+} from the sarcoplasmic reticuli, and even Ca^{2+} overload. In addition, the accumulation of intracellular Na^+ also inhibits the SERCA2 to keep cytosolic $[\text{Ca}^{2+}]_i$ in sustainable elevation (Li et al., 2012), thereby exacerbating Ca^{2+} overload. The most novel finding in our study is that pretreatment with sweroside reversed the aconitine-induced changes of the mRNA transcription of SCN5A, RyR2, DHPR, and SERCA2a, thereby recovering the aberrant alterations of the intracellular Ca^{2+} signals induced by aconitine.

The intracellular calcium overload could enhance intracellular ROS production, which is a well-known driver of cell apoptosis/autophagy or even cell death via the mitochondrial and caspase 3 pathways (Green and Leeuwenburgh, 2002). In this study, we observed that aconitine induced abundant ROS production in H9c2 cells. The augmented ROS directly attacks SERCA2 to decrease its activity, increasing the open probability of RyRs (Xu et al., 1998; Sun et al., 2008) to give rise to $[\text{Ca}^{2+}]_i$ elevation in damaged cells (Di et al., 2016), and then causing arrhythmias by apoptosis (Frey et al., 2000; Gordan et al., 2016; Llano-Diez et al., 2016). Apparently, additional ROS generation and calcium overload promote reciprocally each other, establishing a vicious circle to exacerbate cell damage. The present study revealed that sweroside could break this circle, namely, it simultaneously counteracted aconitine-induced intracellular ROS production and Ca^{2+} elevation, thus protecting the cardiocytes. The cardioprotective mechanism of sweroside on aconitine-induced cell damage was proposed in **Figure 9**.

Autophagy is a dynamic process that turns over organelles and proteins through a lysosome-associated degradation process, and it serves a critical function in cellular homeostasis by regulating cell survival and cell death pathways (Bhandary et al., 2012). Autophagy may promote cell death through excessive self-digestion and the degradation of essential cellular constituents

or it may interact with the apoptotic cascade in the heart (Cao et al., 2009). Many damaged cardiomyocytes show features of autophagic/lysosomal cell death during myocardial injury, including the appearance of cytoplasmic autophagic vacuoles and the recruitment of LC3 to the autophagosomes (Hamacher-Brady et al., 2007). The present study confirmed that aconitine induced autophagy and apoptosis in H9c2 cells by significant increasing LC3- II, cleaved caspase-3 and Beclin-1 expression as well as by decreasing the $\Delta\Psi$. Sweroside, however, could protect H9c2 cells against aconitine-induced autophagy and apoptosis.

In view of the excellent protective effects of sweroside on H9c2 cells, it may be postulated that sweroside could reduce aconitine evoked arrhythmias. Whole rat experiments revealed that sweroside prevented aconitine-induced arrhythmias from deteriorating into lethal types.

In conclusion, the present study revealed that sweroside from *V. baillonii* could ameliorate the aconitine-induced cardiac toxicity *in vitro*, and reduce the arrhythmia incidence induced by aconitine *in vivo*. These results provide a valuable therapy option for the well-known toxin, aconitine. More investigations on the clinical influence of sweroside as well as its mother plants are being conducted in our lab in the future.

AUTHOR CONTRIBUTIONS

L-QM, YY, and X-JH designed the experiments. L-QM, YY, HC, ML, AI, H-YT, X-JH, and YG performed the experiments and analyzed the data. L-QM, YY, and X-JH wrote the paper.

FUNDING

This work was supported by grants from National Natural Science Foundation of China (81873090, 81374064 to X-JH), National Natural Science Foundation of China for Young Scholars (81500253 to L-QM), Qinghai Key Laboratory of Tibetan Medicine Pharmacology and Safety Evaluation, Northwest Institute of Plateau Biology, Chinese Academy of Sciences and Fundamental Research Funds for the Central Universities, South-Central University for Nationalities (CZZ18006 to X-JH, CZY18024 to L-QM). The National Major New Drugs Innovation and Development (2017ZX09301060). The National Natural Science Foundation of State Ethnic Affairs Commission of China (14ZNZ021 to L-QM).

REFERENCES

- Ameri, A. (1998). The effects of Aconitum alkaloids on the central nervous system. *Prog. Neurobiol.* 56, 211–235. doi: 10.1016/S0301-0082(98)00037-9
- Berridge, M. J., Lipp, P., and Bootman, M. D. (2000). The versatility and universality of calcium signalling. *Nat. Rev. Mol. Cell Biol.* 1, 11–21. doi: 10.1038/35036035
- Bhandary, B., Marahatta, A., Kim, H. R., and Chae, H. J. (2012). An involvement of oxidative stress in endoplasmic reticulum stress and its associated diseases. *Int. J. Mol. Sci.* 14, 434–456. doi: 10.3390/ijms14010434
- Cao, D. J., Gillette, T. G., and Hill, J. A. (2009). Cardiomyocyte autophagy: remodeling, repairing, and reconstructing the heart. *Curr. Hypertens. Rep.* 11, 406–411. doi: 10.1007/s11906-009-0070-1
- Carafoli, E. (2002). Calcium signaling: a tale for all seasons. *Proc. Natl. Acad. Sci. U.S.A.* 99, 1115–1122. doi: 10.1073/pnas.032427999
- Catterall, W. A., Trainer, V., and Baden, D. G. (1992). Molecular properties of the sodium channel: a receptor for multiple neurotoxins. *Bull. Soc. Pathol. Exot.* 85(5 Pt 2), 481–485.
- Chan, T. Y. (2009). Aconite poisoning. *Clin. Toxicol.* 47, 279–285. doi: 10.1080/15563650902904407

- Clara, A., Rauch, S., Uberbacher, C. A., Felgenhauer, N., and Druge, G. (2015). High-dose magnesium sulfate in the treatment of aconite poisoning. *Anaesthesist* 64, 381–384. doi: 10.1007/s00101-015-0013-y
- Di, A., Mehta, D., and Malik, A. B. (2016). ROS-activated calcium signaling mechanisms regulating endothelial barrier function. *Cell Calcium* 60, 163–171. doi: 10.1016/j.ceca.2016.02.002
- Fraser, S. P., Salvador, V., Manning, E. A., Mizal, J., Altun, S., Raza, M., et al. (2003). Contribution of functional voltage-gated Na⁺ channel expression to cell behaviors involved in the metastatic cascade in rat prostate cancer: I. lateral motility. *J. Cell. Physiol.* 195, 479–487. doi: 10.1002/jcp.10312
- Frey, N., McKinsey, T. A., and Olson, E. N. (2000). Decoding calcium signals involved in cardiac growth and function. *Nat. Med.* 6, 1221–1227. doi: 10.1038/81321
- Ge, Y. B., Jiang, Y., Zhou, H., Zheng, M., Li, J., Huang, X. J., et al. (2016). Antitoxic effect of *Veratrum baillonii* on the acute toxicity in mice induced by *Aconitum brachypodum*, one of the genus *Aconitum*. *J. Ethnopharmacol.* 179, 27–37. doi: 10.1016/j.jep.2015.12.030
- Gordan, R., Fefelova, N., Gwathmey, J. K., and Xie, L. H. (2016). Involvement of mitochondrial permeability transition pore (mPTP) in cardiac arrhythmias: evidence from cyclophilin D knockout mice. *Cell Calcium* 60, 363–372. doi: 10.1016/j.ceca.2016.09.001
- Gottignies, P., El Hor, T., Tameze, J. K., Lusinga, A. B., Devriendt, J., Lheureux, P., et al. (2009). Successful treatment of monkshood (aconite napel) poisoning with magnesium sulfate. *Am. J. Emerg. Med.* 27, 755.e1–755.e4. doi: 10.1016/j.ajem.2008.10.008
- Green, P. S., and Leeuwenburgh, C. (2002). Mitochondrial dysfunction is an early indicator of doxorubicin-induced apoptosis. *Biochim. Biophys. Acta* 1588, 94–101. doi: 10.1016/S0925-4439(02)00144-8
- Greiser, M., and Schotten, U. (2013). Dynamic remodeling of intracellular Ca²⁺(+) signaling during atrial fibrillation. *J. Mol. Cell. Cardiol.* 58, 134–142. doi: 10.1016/j.yjmcc.2012.12.020
- Hamacher-Brady, A., Brady, N. R., Logue, S. E., Sayen, M. R., Jinno, M., Kirshenbaum, L. A., et al. (2007). Response to myocardial ischemia/reperfusion injury involves Bnip3 and autophagy. *Cell Death Differ.* 14, 146–157. doi: 10.1038/sj.cdd.4401936
- Herzog, W. H., Feibel, R. M., and Bryant, S. H. (1964). The effect of aconitine on the giant axon of the squid. *J. Gen. Physiol.* 47, 719–733. doi: 10.1085/jgp.47.4.719
- Hikino, H., Konno, C., Takata, H., Yamada, Y., Yamada, C., Ohizumi, Y., et al. (1980). Antiinflammatory principles of *Aconitum* roots. *J. Pharmacobiodyn.* 3, 514–525. doi: 10.1248/bpb1978.3.514
- Honerjager, P., and Meissner, A. (1983). The positive inotropic effect of aconitine. *Naunyn Schmiedebergs Arch. Pharmacol.* 322, 49–58.
- Huang, X. J., Li, J., Mei, Z. Y., and Chen, G. (2016). Gentiopicroside and sweroside from *Veratrum baillonii* Franch. induce phosphorylation of Akt and suppress Pck1 expression in hepatoma cells. *Biochem. Cell Biol.* 94, 270–278. doi: 10.1139/bcb-2015-0173
- Li, L., Louch, W. E., Niederer, S. A., Aronsen, J. M., Christensen, G., Sejersted, O. M., et al. (2012). Sodium accumulation in SERCA knockout-induced heart failure. *Biophys. J.* 102, 2039–2048. doi: 10.1016/j.bpj.2012.03.045
- Lin, C. C., Chan, T. Y., and Deng, J. F. (2004). Clinical features and management of herb-induced aconitine poisoning. *Ann. Emerg. Med.* 43, 574–579. doi: 10.1016/j.annemergmed.2003.10.046
- Llano-Diez, M., Cheng, A. J., Jonsson, W., Ivarsson, N., Westerblad, H., Sun, V., et al. (2016). Impaired Ca²⁺ release contributes to muscle weakness in a rat model of critical illness myopathy. *Crit. Care* 20:254. doi: 10.1186/s13054-016-1417-z
- Naranjo, J. R., and Mellstrom, B. (2012). Ca²⁺-dependent transcriptional control of Ca²⁺ homeostasis. *J. Biol. Chem.* 287, 31674–31680. doi: 10.1074/jbc.R112.384982
- Sato, H., Yamada, C., Konno, C., Ohizumi, Y., Endo, K., and Hikino, H. (1979). Pharmacological actions of aconitine alkaloids. *Tohoku J. Exp. Med.* 128, 175–187. doi: 10.1620/tjem.128.175
- Sawanobori, T., Hirano, Y., and Hiraoka, M. (1987). Aconitine-induced delayed afterdepolarization in frog atrium and guinea pig papillary muscles in the presence of low concentrations of Ca²⁺. *Jpn. J. Physiol.* 37, 59–79. doi: 10.2170/jphysiol.37.59
- Sun, J., Yamaguchi, N., Xu, L., Eu, J. P., Stamler, J. S., and Meissner, G. (2008). Regulation of the cardiac muscle ryanodine receptor by O(2) tension and S-nitrosoglutathione. *Biochemistry* 47, 13985–13990. doi: 10.1021/bi8012627
- Wright, S. N. (2002). Comparison of aconitine-modified human heart (hH1) and rat skeletal (mu1) muscle Na⁺ channels: an important role for external Na⁺ ions. *J. Physiol.* 538(Pt 3), 759–771.
- Xu, L., Eu, J. P., Meissner, G., and Stamler, J. S. (1998). Activation of the cardiac calcium release channel (ryanodine receptor) by poly-S-nitrosylation. *Science* 279, 234–237. doi: 10.1126/science.279.5348.234
- Yang, Y. B., and Zhou, J. (1980). [Studies on the xanthones of *Veratrum baillonii* Franch. I. Structures of veratriloside and veratrilogenin (author's transl)]. *Yao Xue Xue Bao* 15, 625–629.
- Yeih, D. F., Chiang, F. T., and Huang, S. K. (2000). Successful treatment of aconitine induced life threatening ventricular tachyarrhythmia with amiodarone. *Heart* 84:E8. doi: 10.1136/heart.84.4.e8
- Yu, Y., Yi, X. J., Mei, Z. Y., Li, J., Huang, X. J., Yang, G. Z., et al. (2016). The water extract of *Veratrum baillonii* could attenuate the subacute toxicity induced by *Aconitum brachypodum*. *Phytomedicine* 23, 1591–1598. doi: 10.1016/j.phymed.2016.10.001
- Zhou, Y. H., Piao, X. M., Liu, X., Liang, H. H., Wang, L. M., Xiong, X. H., et al. (2013). Arrhythmogenesis toxicity of aconitine is related to intracellular Ca²⁺ signals. *Int. J. Med. Sci.* 10, 1242–1249. doi: 10.7150/ijms.6541

Conflict of Interest Statement: The authors declare that the research was conducted in the absence of any commercial or financial relationships that could be construed as a potential conflict of interest.

Copyright © 2018 Ma, Yu, Chen, Li, Ihsan, Tong, Huang and Gao. This is an open-access article distributed under the terms of the Creative Commons Attribution License (CC BY). The use, distribution or reproduction in other forums is permitted, provided the original author(s) and the copyright owner(s) are credited and that the original publication in this journal is cited, in accordance with accepted academic practice. No use, distribution or reproduction is permitted which does not comply with these terms.